Heat transfer characteristics and flow visualization of anodized flat thermosiphon

Allen Varughese[a], A. Brusly Solomon[a,*], Benny Raj[a], Mohsen Sharifpur[b], Josua P. Meyer[b]

[a]Centre for Research in Material Science and Thermal Management, Department of Mechanical Engineering, Karunya Institute of Technology and Sciences, Coimbatore, India.

[b]Department of Mechanical and Aeronautical Engineering, University of Pretoria, Hatfield, 0028, Pretoria, South Africa.

Corresponding author*

Dr. A. Brusly Solomon, M.E., Ph.D.,
Associate Professor,
Department of Mechanical Engineering,
Karunya Institute of Technology and Sciences.
Coimbatore – 641 114
Tel: 0422-2614059
Mobile: 8220023860
Email: abruslysolomon@gmail.com

Acknowledgment

The authors would like to acknowledge the DST-SERB (Project number YSS/2015/001084) for financial assistance to conduct this research.

Abstract

Use of environmentally safe refrigerants is the need of the hour to minimize the carbon footprints and to reduce the ozone depletion. The application of such environmentally safe refrigerants in the thermosyphon with the micro/nanoporous coating is expected to operate efficiently. In this study, a simple cost effective anodizing technique to form a uniform thin micro/nano-porous coating at the inner wall of the thermosiphon is undertaken, and the resulting performance enhancement is presented. Also, the effect of fill ratio, heat input and the porous coating on the heat transfer characteristics of flat thermosiphon are studied. The heat transfer coefficient in the evaporator of anodized and non-anodized thermosiphon is enhanced to a maximum of 3587 and 2742 $W/m^2 K$ respectively. The number of pores present in the anodized evaporator surface is estimated as 3.4 x 10^9. The width (pore size) and depth of pore are measured as 0.25 µm and 16nm respectively. The porosity of the coating is around 55%, and the contact angle is $\leq 10^o$. As a result, the heat transfer coefficient at the evaporator and condenser of anodized thermosyphon is enhanced to a maximum of 24 and 13% respectively, when compared to that of the non-anodized thermosiphon.

Keywords: Anodized thermosiphon; Heat transfer enhancement; Nucleate boiling; Visualization, porous coating

1. INTRODUCTION

Thermosiphon is a two-phase heat transfer device which works based on boiling and condensation process, and it can transfer a huge amount of heat over a considerable distance with a small temperature drop. This high heat transfer is achieved by the latent heat exchange process in the evaporator and condenser. Much attention was given to the design of evaporator and condenser to improve the effectiveness of the same. It is known that the boiling phenomenon in the evaporator section of thermosiphon is an important and essential process for continuous operation. As a result,

several studies have been directed to study of the nucleate boiling characteristics and to understand the mechanism behind the heat transfer enhancement especially to understand the process of nucleation, bubble growth, and departure. However, this still remains one of the least understood topics of thermal engineering due to a number of interlinked complex processes. It is well known that the nucleation occurrence depends on the topography of the surface, properties of the solid and liquid as well as operating parameters like pressure and temperature. It was observed that artificial nucleation sites of appropriate design depending on the solid-liquid combination could enhance the rate of heat transfer substantially in nucleate boiling [1].

The study of boiling phenomenon continues to be of immense importance to researchers. The nucleation sites help to reduce the wall superheat and extend the critical heat flux occurring. In the last few decades, the use of nanofluids to increase heat transfer was received much attention, and few investigations have shown that the use of nanofluids leads to blocking of nucleation sites thereby having the opposite effect and reducing the heat transfer [2, 3]. Later, heat transfer in artificially enhanced micro-pores on the evaporator section was performed [4, 5] and found that the heat transfer coefficient was increased by about 20-30%. Consequently, more studies were carried out to develop such surfaces and to study heat transfer performance. Teodori et al. [6] conducted a pool boiling study with micro-textured surface and studied the effects of distance between the micro-pores on the heat transfer coefficient. Lee et al. [7] reported an increase in heat transfer coefficient in a pool boiling study by creating micropores in aluminium workpiece by the anodizing process. Kumar et al. [8] studied the pool boiling heat transfer characteristics of a surface with different diameters of copper nanowires ranging from 35 - 200 nm. Demir et al. [9] studied the pool boiling heat transfer of a Si nanostructured surfaces consist of the nanorod. A similar pool boiling study conducted by Chen et al. [10] showed that the nanowires of Si and Cu coated on the substrate enhanced the thermal conductance and critical heat flux more than 100% compared to the surface without nanowires. Yao et al. [11] studied the pool boiling heat transfer in a Silicon microchannels coated with Silicon Nanowires.

Surtaev et al. [12] studied the pool boiling heat transfer behavior of a capillary porous coating using water and liquid nitrogen as a coolant at atmospheric conditions. Deng et al. [13] made a comparative study of pool boiling heat transfer using a reentrant Ω shaped channel made of porous coating and with a solid sample of the same dimension. Ahmad et al. [14] studied the saturated pool boiling performance of copper surfaces modified with different treatments such as emery-polished surface, a finely sandblasted surface, a rough sandblasted surface, an electron beam-enhanced surface, and a sintered surface. Above studies [8-14], clearly indicates that the micro/nanoporous coatings enhance the boiling heat transfer significantly when compared to the ordinary surfaces and the need for improving the surface for heat transfer.

Khodabandeh et al. [15] found that the micropore structures formed at the inner evaporator side of the thermosiphon was increased the heat transfer coefficient of the evaporator by 9%, and also it reduced the instability during the boiling process. Krishnan et al. [16] formed a metallic copper nanowire at the evaporator of a miniature loop heat pipe and found that the heat transfer coefficient was 2.7 times higher than that of the same without nanowire. Chen et al. [17] studied the scale effect on the heat transfer coefficient of the heat pipe with carbon nanotube (CNT) as a wick structure. This study revealed that the nanopore between the CNT develops a high capillary pressure. Ling et al. [18] modified the wick structure of loop heat pipe by incorporating the rough porous copper fiber sintered sheets (PCFSS) and studied the performance of the same by varying the fill ratio and morphology of the wick surface. It was found that the addition of PCFSS reduces thermal resistance. The PCFSS with a porosity of 70% and fill ratio of 30% found to be an optimum condition which helped the heat pipe to operate between 5-200W. Buffone et al. [19] developed a graphene-based wick structure for loop heat pipe applicable for aeronautics, in which graphene oxide particles were coated on the surface of nickel sintered powder wick that is facing towards the vapour and found that the capillary pressure was enhanced 3.5 times higher than that of the nickel sintered powder wick. Choi et al. [20] developed a wick structure suitable for loop heat pipes by sintering a thin copper nanoparticles film on the

microporous copper substrate by low-temperature sintering. It was found that the capillary pressure of the wick was enhanced twice by the thin Nanoporous coating compared to that of without Nano coating.

Lee et al. [21] studied the performance of oxidized aluminium thermosiphon with water as the working fluid and noticed a formation of the hydroxide layer in the aluminium base material. As a result, the efficiency of thermosiphon reduced drastically over time. Solomon et al. [22] compared the heat transfer characteristics of non-anodized and anodized thermosiphon with acetone as working fluid. The heat transfer coefficient of anodized thermosiphon was found to be enhanced by 15-20% of the same of non-anodized thermosiphon. Also, it is noticed that the evaporator heat transfer coefficient was increased significantly. On the other hand, the same as the condenser was increased marginally. A similar enhancement in heat transfer was found in the previous studies [23-26] while testing heat pipes and thermosiphon with the thin porous coating.

From the above studies, it was found that the surface of evaporator has immense significance on the heat transfer enhancement. Artificial micro/nanopores of the evaporator section would lead to an increase in a number of nucleation site resulting in enhanced heat transfer performance. Therefore the previous studies [23-26] deliberate the effect of nucleation sites on the performance enhancement resulting from the boiling enhancement while testing with different working fluids. However, the present study deliberates the effect of nucleation sites on the boiling heat transfer as well as the variation in the condensation process in the flat anodized thermosyphon. Also, this study brings out more evidence of bubble formation and condensate flow which has rarely been reported in other literature especially for the anodized surfaces.

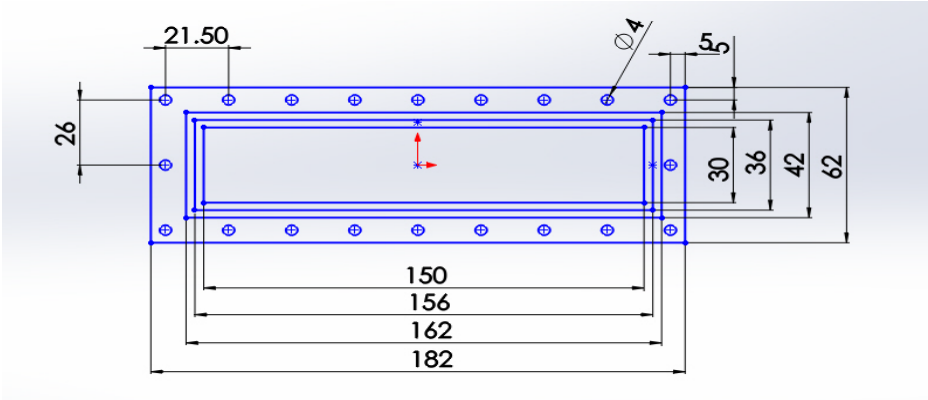

(a)

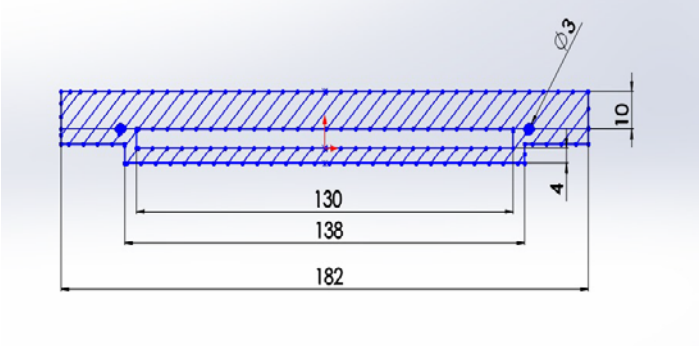

(b)

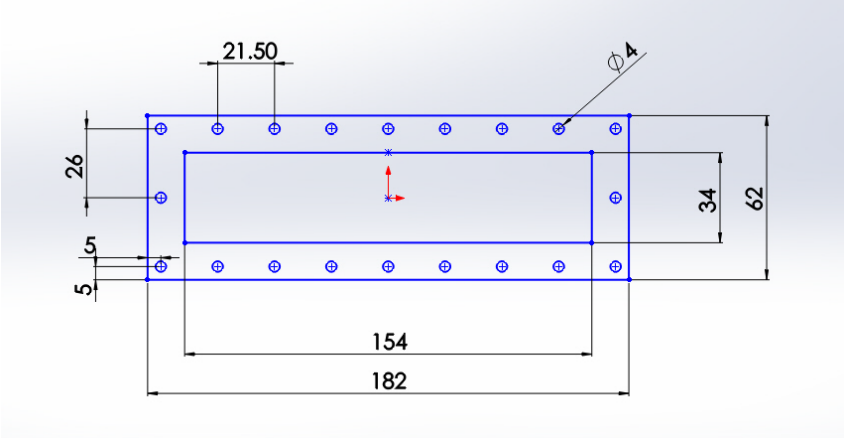

(c)

Fig. 1 Sketch of the fabricated heat pipe (a) Top view (b) sectional view and (c) bottom views (all dimensions are in mm)

2. Experimental Details

2.1 Fabrication of Heat pipe

In this study, thermosiphon is fabricated to visualize the boiling process of the heat pipe. Therefore it is fabricated with two parts, namely, ie. Aluminium base (thermosiphon material) and acrylic top. The aluminium base is made by machining an aluminium block with the dimension of 182mm length, 62mm width, and 9mm thick. The top view, sectional and bottom view of the machined thermosiphon with all necessary dimension is shown in Fig 1 (1), (b) and (c) respectively. At the center of the aluminium block, machining is done to make a rectangular cavity with dimensions of 150mm length, 30mm width and a depth of 5mm. After that, the diameter of 3mm semi-cylindrical groove is machined around the cavity, which is 3mm from the outer edge of the cavity made earlier, in order to accommodate the O-ring which acts as a seal inside the thermosiphon. There are 20 number of holes with the diameter of 4mm drilled around the cavity at a distance of 3mm from the outer edge of the groove or from the outer edge of the aluminium block. Now, the bottom surface of the aluminium block is machined in such a way that all sides of the cavity have a wall thickness of 4mm. After the necessary cleaning process, the aluminium base is covered with 10mm thick acrylic plate for visualization. The acrylic plate is also machined to a dimension of 182 mm length, 62 mm width and 10 mm thickness. Then, 20 numbers of 4mm diameter holes to match with the thermosiphon enclosure are machined. In order to maintain a sufficient vacuum, aluminium base and acrylic top are sealed with rubber O-ring.

2.2 Anodization

The anodization process is performed in an aluminium base (later used as thermosiphon enclosure) as the anode and stainless steel plate as the cathode. Oxidation occurs at anode and aluminium oxide is formed at aluminium surface. This coating is of micro/nanoscale, and this would help in increasing the number of nucleation site and enhance the heat transfer. Sulphuric acid is taken as the electrolyte with 15 % concentration. The anodization process involves two stages, first the pretreatment and then anodization process. Pretreatment process comprises cleaning the workpiece to get rid of any

accumulated dirt or dust particle. Then it is dipped in a solution of caustic soda (NaOH) for two minutes so that the outer layer of residues dissolve and removed. This solution of caustic soda (NaOH) is prepared by mixing 50g of sodium hydroxide pellets in one liter of de-ionized water (50gm/liter). Then the workpiece is washed with de-ionized (DI) water for two minutes to remove the NaOH deposits from the workpiece. The workpiece is then immersed in a bath of diluted nitric acid (HNO_3) with a concentration of 10% for removing any unwanted particles and again rinsed with de-ionized water for another two minutes.

The workpiece is then connected to the anode ('+'ve terminal) of the DC supply and immersed in the electrolytic pool. The cathode consists of stainless steel which is connected to the negative terminal of the DC supply. After the test setup was made, DC supply was switched on and the voltage was increased slowly. Voltage was kept at 1V for one minute and then increased a step of one volt after each minute till it reaches 18V. After reaching 18 V, the power was kept constant for about seventy minutes with a current of 1.7 amperes (A). The range of voltage and time required would depend on the area of the workpiece to be coated. After the stipulated time period, the workpiece was taken out and washed again with de-ionized water (DI) to cleanse electrolytic residues on the surface. After the anodizing process, it was noticed that a rough white color coating on the workpiece is developed. This coating was observed using a Scanning Electron Microscope, and it revealed that there are thousands of micro/nanoscale peaks and trough created on the aluminium surface in a uniform manner as shown in Fig 2(b). The number of pores present in the total evaporator is estimated by counting the number of pores present in the 2µm square area and extrapolating it to the entire evaporator area. Moreover, the peak to peak distance of the pore is measured and is 0.25 µm. These pores are supposed to act as nucleation sites during the boiling process and would enhance the heat transfer. The porosity of the anodized surface is calculated using a well-known displacement method. Efforts have been made to measure the wettability of the surface by measuring the contact angle using the Drop Shape Analyzer. However, contact angle measurement was unsuccessful as the surface is

highly wettable due to the hydrophilic nature of the surface in which the liquid spreads quickly and absorbed by the coating. Using the anodized workpiece, thermosiphon is fabricated and charged with an environment-friendly refrigerant R600a, since it has a low vapor pressure compared to other refrigerants. This property is essential for performing visualization study using the acrylic sheet at the top of the evaporator. In the beginning, the fill ratio of thermosiphon is kept at 100% by filling the entire evaporator section with working fluid. Later after every test, the fill ratio is varied by opening the charging valve and releasing the refrigerant. The quantity of the refrigerant required for each fill ratio is ensured by weighing the thermosiphon.

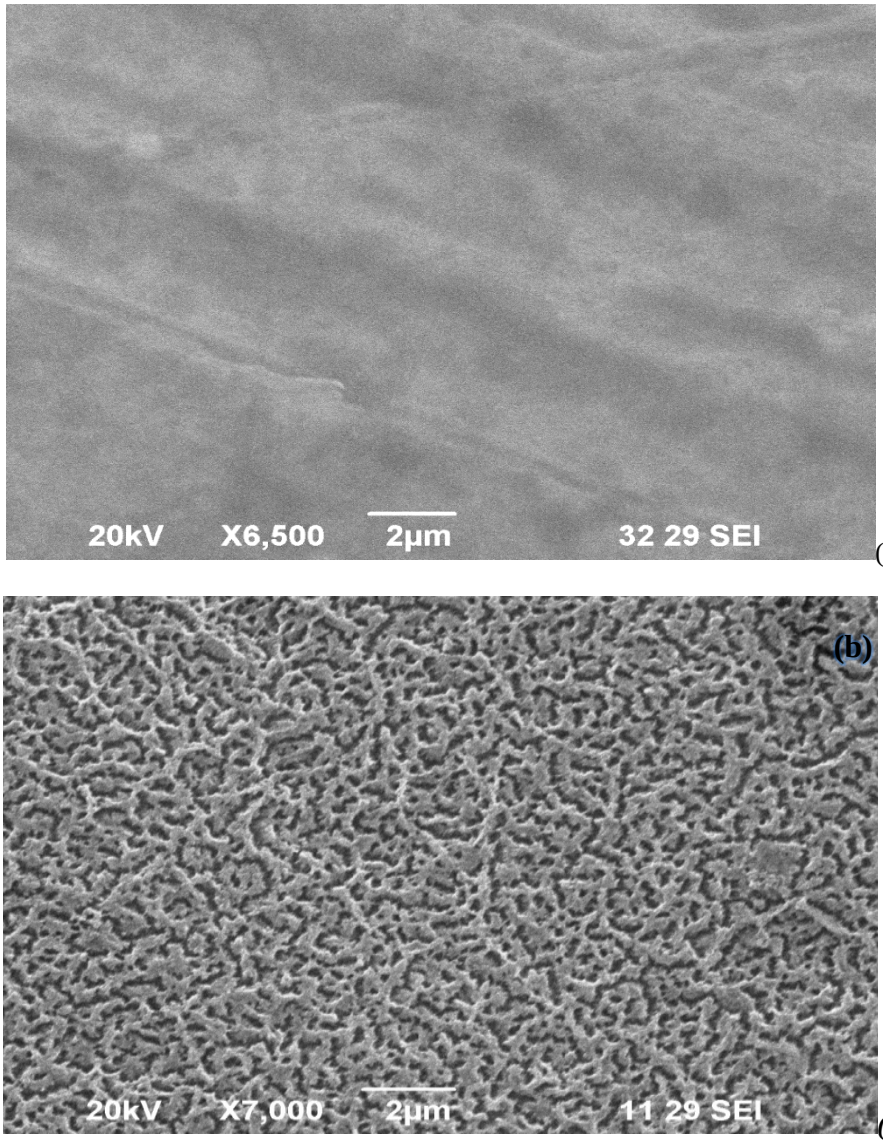

Fig.2 SEM image of (a) non anodized and (b) anodized aluminium test piece

2.3 Experimental procedure

The schematic experimental setup of the present study is shown in Fig .3(a) and it consists of the thermosiphon kept in a vertical position (shown in the Fig. 4), data logger, DC supply, chiller, and a flow meter. The thermosiphon was divided into three sections namely evaporator, adiabatic and condenser section. Generally the size of the evaporator is fixed based on the size of the heat source and the condenser size is fixed as 1.5 times or twice the size of evaporator to maximize the heat transfer. In this study, top 80mm length of the thermosiphon was considered as a condenser section. Cooling water from the chiller was supplied to the duct which was attached at the backside of the condenser, and thereby the cooling is provided. The bottom-most 40mm of the thermosiphon is considered as evaporator where heat input is given to the thermosiphon. A cartridge heater inserted into the copper block is used to supply the heat input. The heater is connected with a variable transformer in which the current and voltage are controlled. The portion between the evaporator and condenser is called an adiabatic region which acts as a transport section. Thick insulation was provided around the adiabatic region to prevent any heat loss to the surrounding. There were three T-type thermocouples each in the evaporator and condenser respectively, and the same type of two thermocouples in the adiabatic section was welded as shown in Fig 3. The accuracy of the thermocouple including the accuracy of data logger (Agilent, Model: 34972A) given by the manufactures was $\pm 0.2^{o}$C. The uncertainty present in the coolant flow rate at the condenser section was ±3%. When the steady-state was obtained after each heat input the boiling process and the condensate return was captured using a Canon EOS 600D camera.

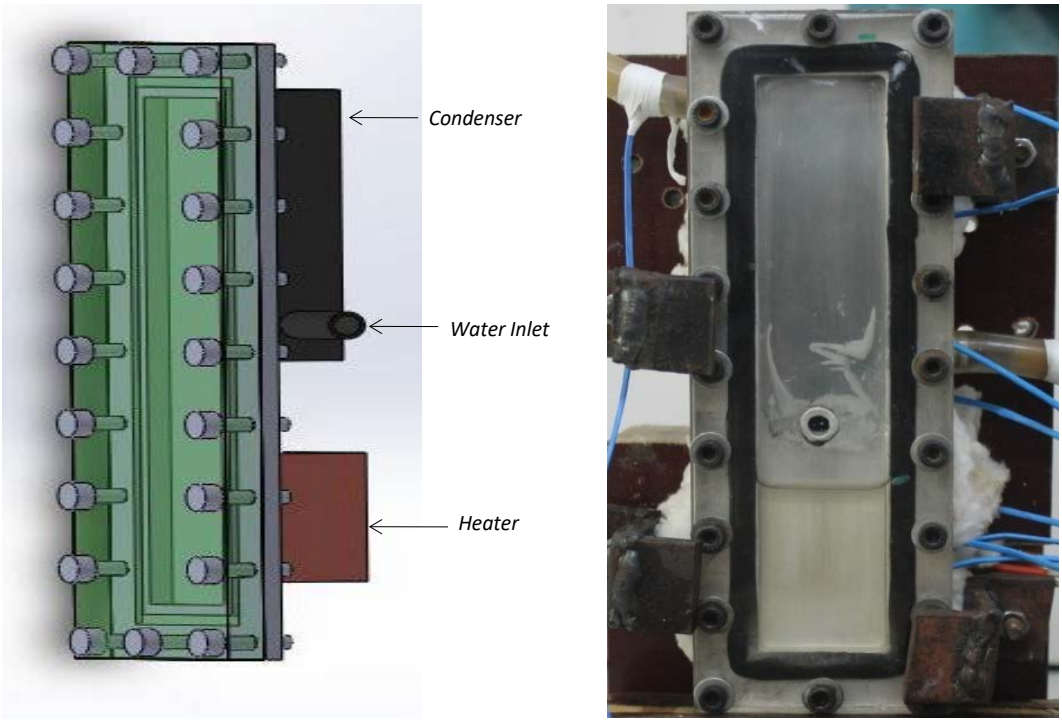

Fig. 4 View of thermosyphon (a) model and (b) after charging the working fluid

2.4 Data reduction

Heat transferred by the thermosiphon is calculated using Newton's law of cooling as shown in equation (1) and the heat supplied to the evaporator is calculated by multiplying the voltage, and current supplied to the cartridge heater as given in equation (2)

$$\dot{Q_{out}} = \dot{m}\, C_p\, (T_{out} - T_{in}) \tag{1}$$

$$\dot{Q}_{in} = V\ x\ I \tag{2}$$

The total thermal resistance R_t calculated by:

$$R_T = \frac{\Delta T}{Q_{out}} \tag{3}$$

where $\Delta T = \bar{T}_e - \bar{T}_c$

The heat transfer coefficient of the evaporator (h_e) and condenser (h_c) are calculated by the equations (4) and (5) as:

$$h_e = \frac{q_e}{T_e - T_{sat}} \quad (4)$$

$$h_c = \frac{q_c}{T_{sat} - T_c} \quad (5)$$

where q_e and q_c are heat influx at evaporator and condenser section.

At last, the uncertainty present in heat flux, heat transfer coefficient, and thermal resistance are calculated based on the previous studies [22,23,25,26]. The calculated uncertainties in the measurements of heat flux, heat transfer coefficient, and the total resistance are presented in Table 1 and found to be less than 7% which is within an acceptable limit.

Table 1 **Uncertainty in the estimation of heat transfer coefficient and Total resistance**

Heat input (W)	Uncertainty (%)				
	Heat transfer coefficient				Resistance
	Non-Anodized		Anodized		
	Evaporator	condenser	Evaporator	Condenser	
10	4.51	7.48	5.34	6.22	3.42
20	3.55	5.15	4.15	5.48	2.91
30	3.19	4.32	3.61	5.05	2.74
40	3.00	3.89	3.31	4.24	2.67
50	2.82	3.49	3.01	3.62	2.61

3. Results and Discussion

Experiments are carried out to study the heat transfer characteristics of anodized thermosiphon using R600a as the working fluid. The experimental investigation is undertaken by two series of testing. The first series of testing performed to study the heat transfer characteristics of non-anodized thermosiphon as well as to identify the optimum fill ratio for maximum heat transfer and the second series of testing is performed to study the effect of coating in anodized thermosiphon with the optimum fill ratio obtained from the first series of testing. The fill ratio of the thermosiphon is varied from 40-100% of the evaporator volume of the thermosiphon. Heat input is varied between 10-50W. Apart from the performance study, the boiling process of both anodized and non-anodized thermosiphon was recorded and presented.

Fig. 5 shows the evaporator, adiabatic and condenser wall temperature of thermosiphon with different fill ratio of working fluid. It is seen that the wall temperature is increasing as the heat input increases in all the sections of thermosiphon. Also, noticed that the temperature at the evaporator, adiabatic and condenser sections are varying between 30-70 ^{o}C, 23-47 ^{o}C, and 20-38 ^{o}C, respectively for the heat input range of 10-50W. Moreover, the wall temperature variation concerning different fill ratio is insignificant at lower heat inputs and significant at higher heat inputs. To identify the optimum fill ratio, the individual thermal resistance of evaporator and condenser, as well as the overall thermal resistance are calculated and presented.

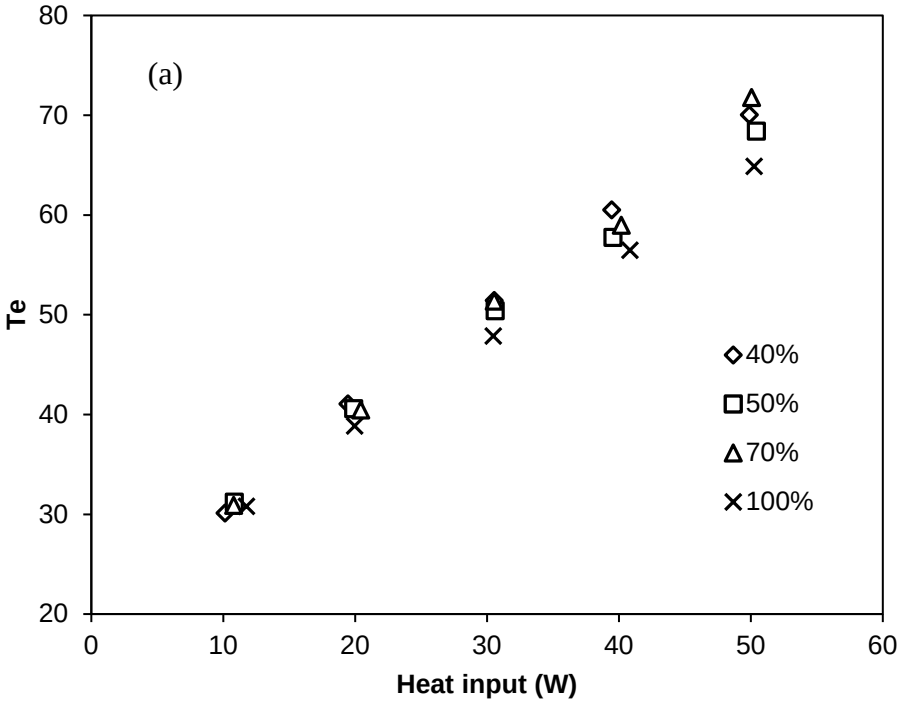

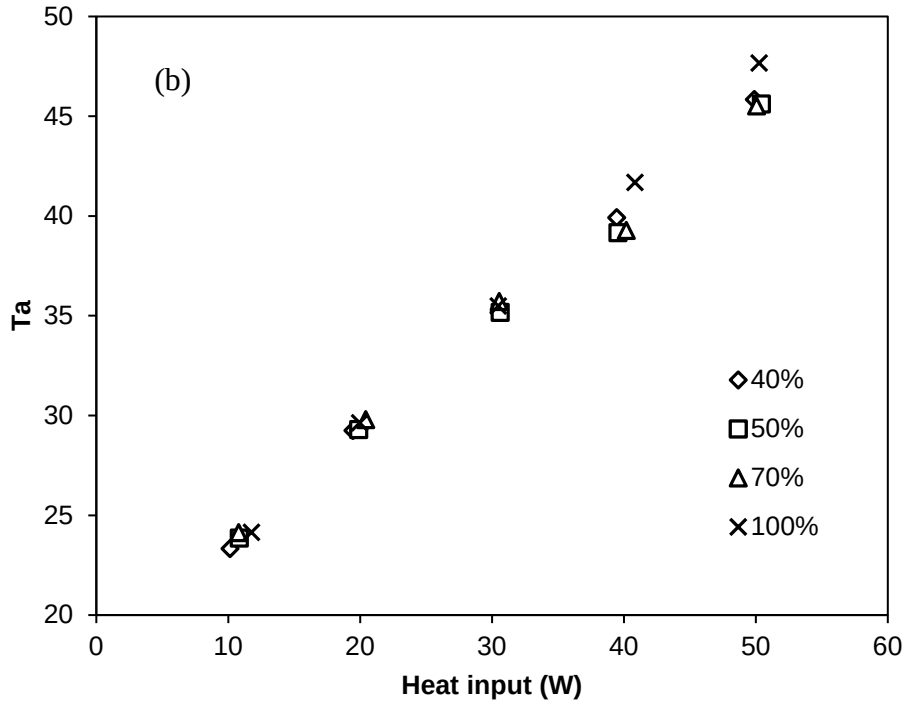

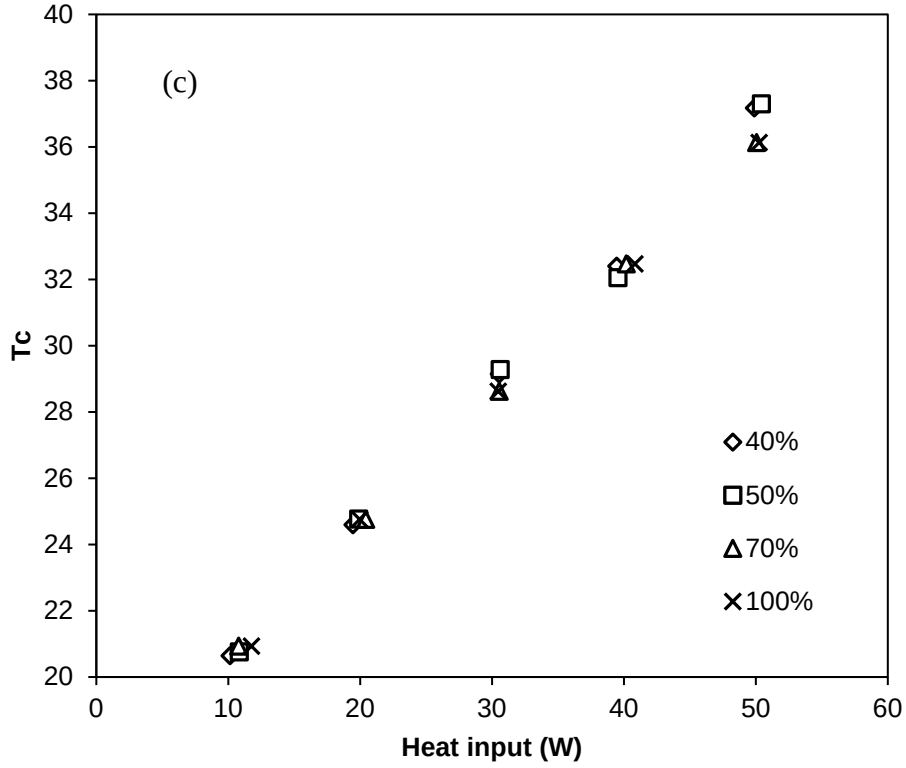

Fig. 5 Wall temperature variations at (a) Evaporator (b) Adiabatic and (c) Condenser sections of the non-anodized thermosiphon

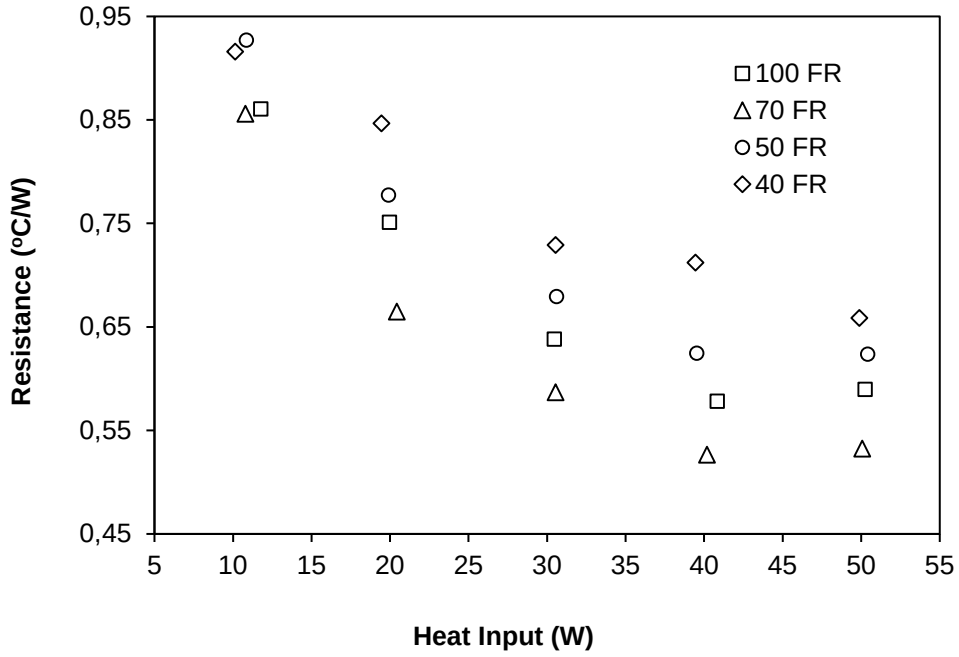

Fig. 6 Effect of heat input on the thermal resistance of non-anodized thermosiphon for various fill ratios

The overall thermal resistance is calculated using equation (3) and presented in Fig.6 and it reveals that the overall thermal resistance decreases with the increasing heat input and steadies afterwards. It is well-known that the boiling performance enhances as the heat input increases resulting in decreasing resistance. It is also noticed that the thermal resistance is influenced by the fill ratio of the working fluid. The thermosiphon charged with a fill ratio of 70% working fluid showed a minimum thermal resistance as compared to the other fill ratios. This low resistance may be obtained due to the effective return of working fluid from condenser to evaporator, optimum pool height and continuous wetting of evaporator as well as boiling mechanism. The excess pool height at 100% fill ratio, put additional pressure on the boiling surface and reduce the heat transfer leading to higher resistance. On the other hand, lower liquid pool height at low fill ratio leads to the formation of hot spots due to inadequate liquid inventory in evaporator leading to high incipient wall superheat and higher resistance. Also, it is noticed that the thermal resistance at 10 W is 0.92 (^{0}C/W) and it reduces to 0.61(^{0}C/W) when the heat input is 40W for the thermosiphon with 70% fill ratio. So a decreasing trend is seen from 10 to 40W. However, a further increase in the heat input leads to the increase in

resistance and attains value 0.64(^{0}C/W) at 50 W. This increase in resistance may be caused due to the change in boiling dynamics in the evaporator region. At low heat fluxes, heat transfer occurs by both conduction and convection heat transfer mechanism and as the heat fluxes increases, nucleate boiling occurs and resulted in resistance reduction. Further, an increase in heat flux leads to the formation of film boiling which is less effective than nucleate boiling leading to the higher resistance. Moreover, it is economical to use 70% fill ratio as an additional increase in working fluid does not contribute to a reduction in thermal resistance.

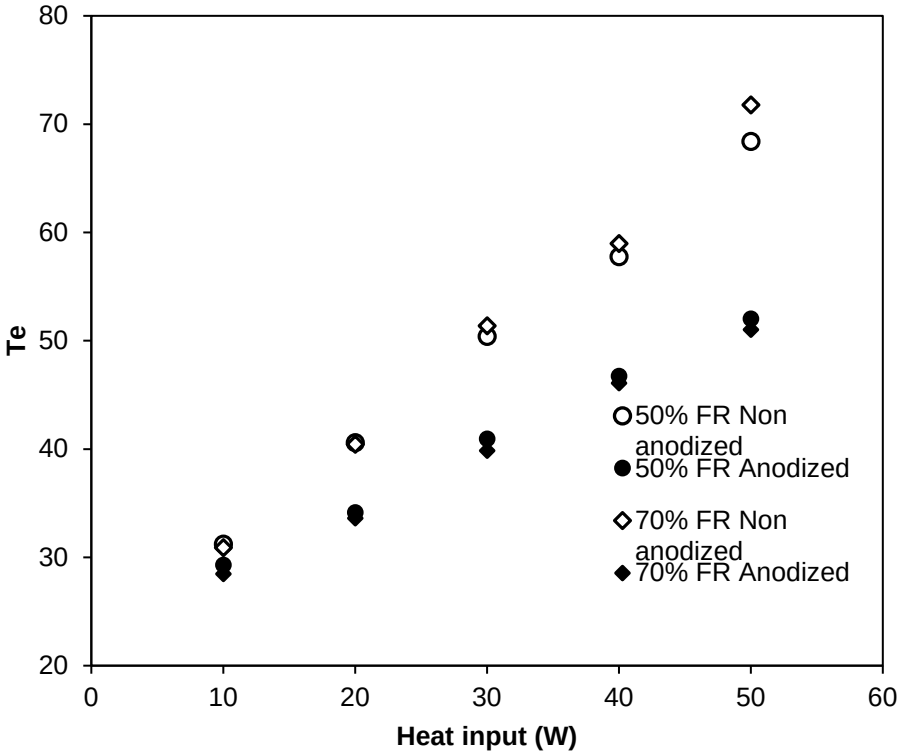

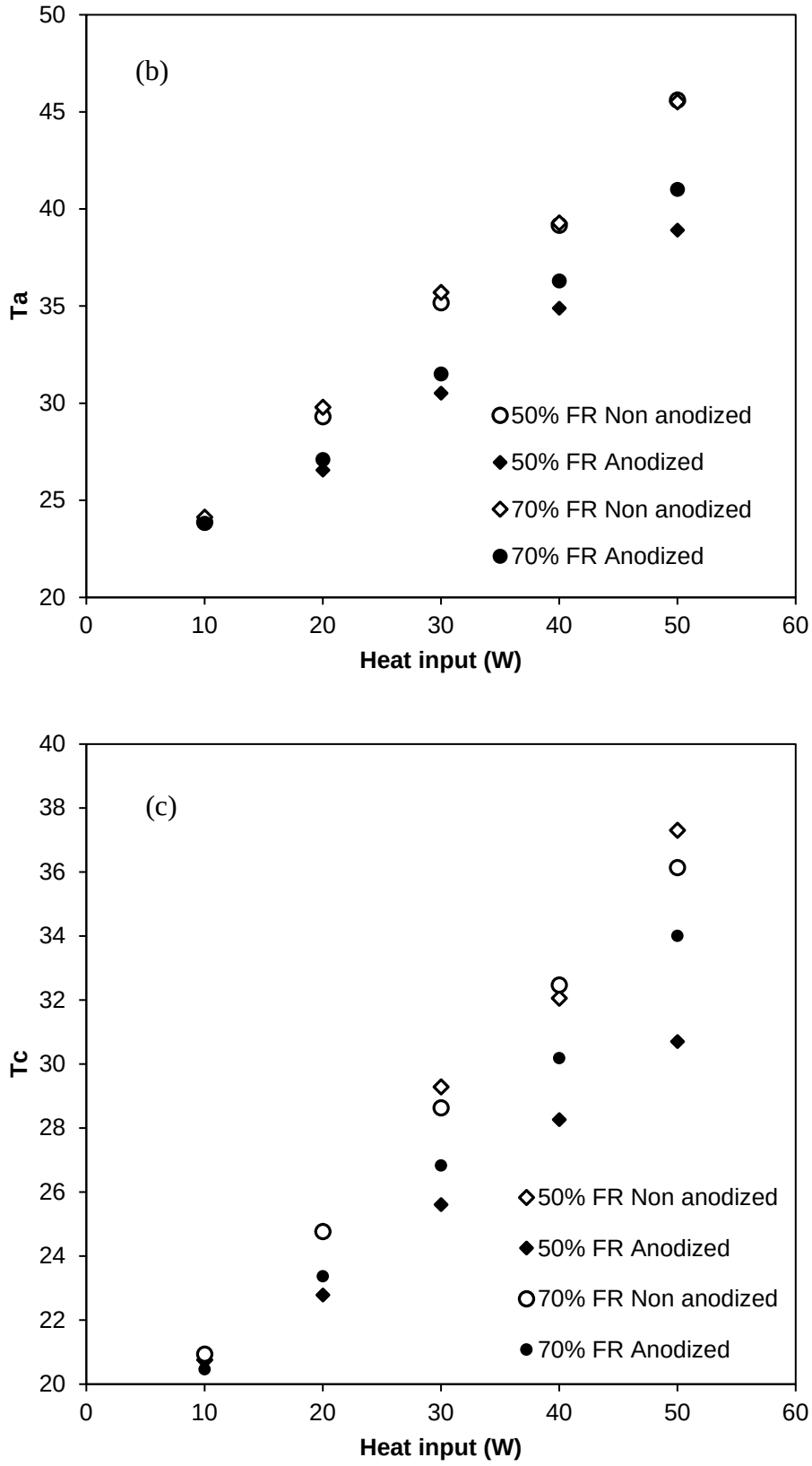

Fig. 7 Effect of heat input on the wall temperature of (a) evaporator (b) Adiabatic and (c) Condenser section for non-anodized and anodized thermosyphon.

Fig. 7 shows the wall temperature variation at the evaporator, adiabatic and condenser of anodized and non-anodized thermosiphon at various heat inputs for 50% and 70% fill ratio. The above fill ratio was presented only because of both showed a low thermal resistance. From the figure, it is seen that the wall temperature of the anodized thermosiphon is significantly reduced due to the coating when compared to the non-anodized case. This variation is resulted from the boiling enhancement due to the change in surface morphology of the coated surface. It is noted that the anodized surface consists of large numbers of micro/nanopores, as shown in Fig 2, which act as nucleation sites and enhance the nucleate boiling. To explain this variation, the number of pores which act as nucleation sites present in the evaporator is estimated for the anodized surface is $3.4x10^9$, however, there are no such pores noticed in the non-anodized surface (polished surface). Further, the pore size (width) and depth of pore for the anodized surface was also measured from the SEM image and are 0.25 μm and 16nm respectively. The porosity of the coating is found to be around 55%, and the contact angle is $\leq 10^o$. The presence of such additional nano/micro-sized nucleation sites with the above property in the anodized surface reduces the incipient wall superheat by promoting nucleate boiling leading to the better heat transfer and low resistance. The lower contact angle and porous formation due to the coating help the heat transfer surface remain wet and saturated with working fluid also leads to low incipient wall superheat. Therefore, boiling heat transfer in the anodized surface is better than the non-anodized surface leading to the reduction in incipient wall superheat [27]. Thus the low temperature is obtained in the evaporator. Also, it is clear that the difference between the wall temperature of both anodized and non-anodized case is increasing with heat input. This increase in wall temperature difference is due to the activation of additional nucleation sites. It is known that the nucleation sites are activated as the heat flux increases leading to the better boiling in the anodized surface. Though the nucleation sites are opened in both anodized and non-anodized surface, number of nucleation sites are activated in the anodized surface than in the non-anodized surface. Therefore,

the anodized surface outperforming the non-anodized case leading to an increase in temperature difference. More information in this regard is found in the previous studies [23-26].

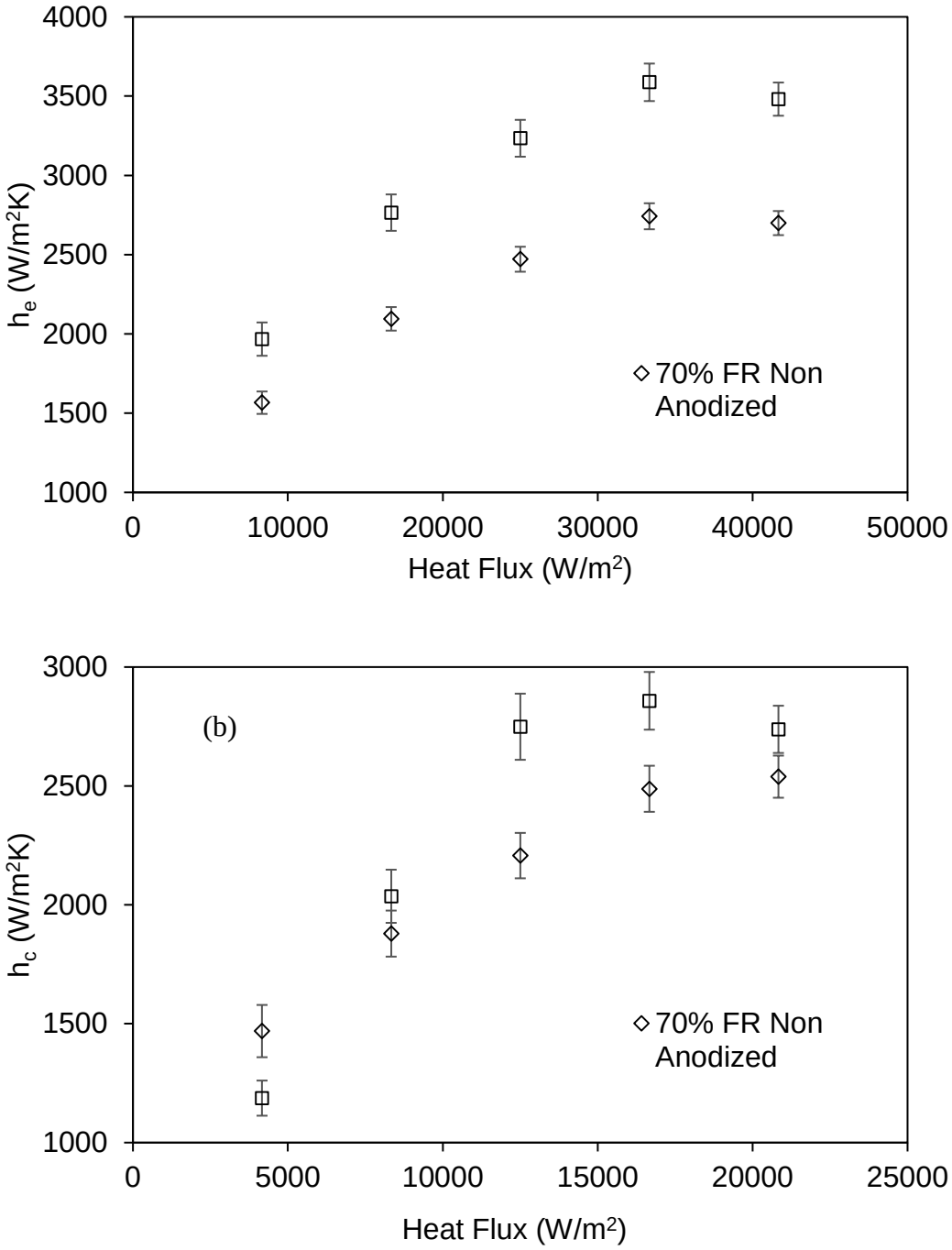

Fig. 8 Effect of heat flux on (a) evaporator and (b) condenser heat transfer co-efficient for non-anodized and anodized thermosiphon.

Fig. 8(a,b) shows the variation of the heat transfer coefficient of both anodized and non-anodized thermosiphon with 70% fill ratio. As expected, the heat transfer coefficient of both

evaporator and condenser is increasing with heat input up to 40W, and then it starts decreasing at 50W. The captured liquid pool is presented in Fig. 9, and it shows that the pool height is decreasing as the heat input increases for both non-anodized and anodized thermosiphon leading to the increase in heat transfer coefficient. The pool height variation depends on the rate of boiling and condensation. The decreasing trend in pool height suggests that the rate of boiling and condensation increasing with heat input. Moreover, the intensity of the boiling found to be increasing as the heat input increases. Also, it is noticed that the heat transfer coefficient of anodized thermosiphon is higher than the non-

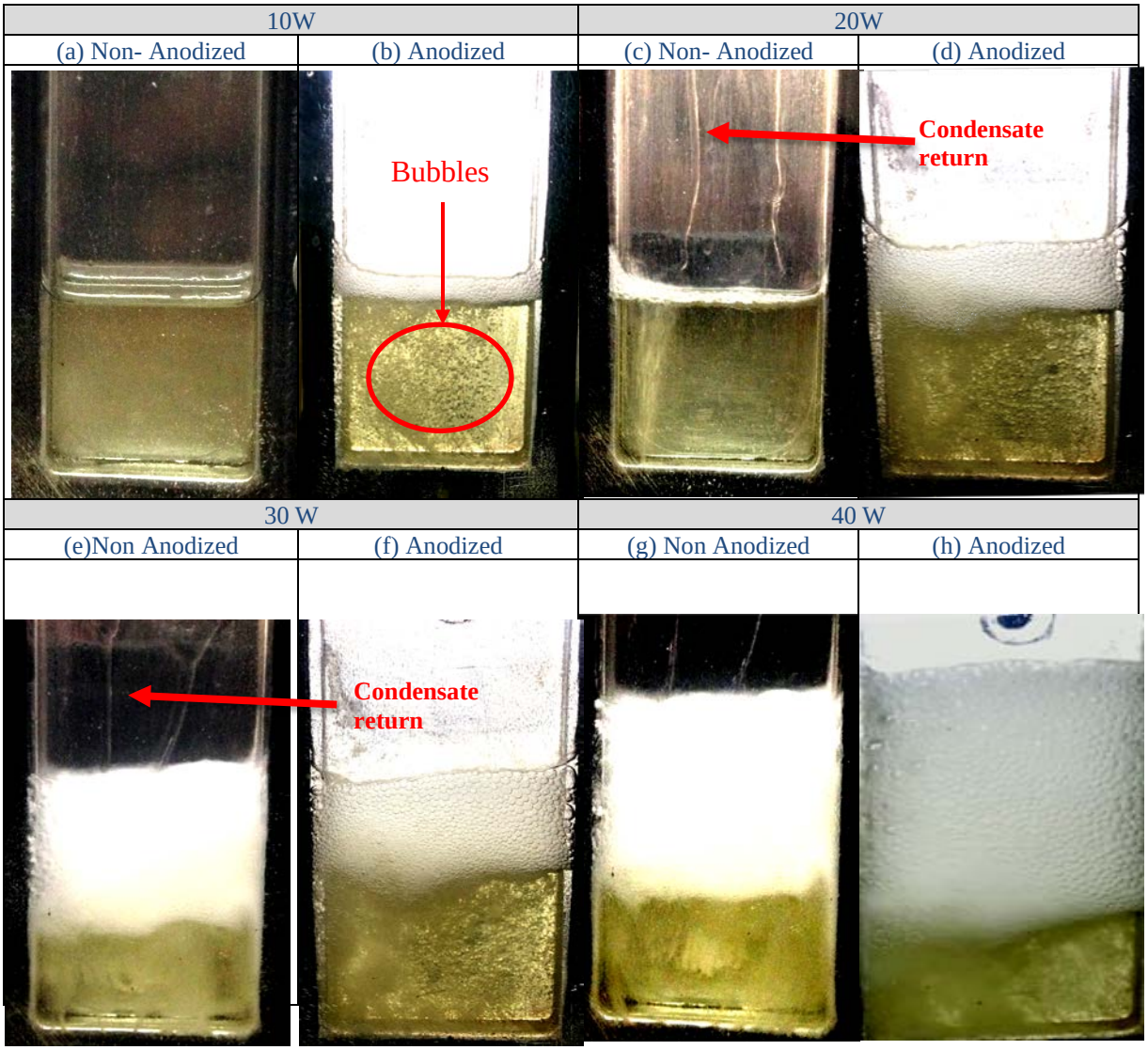

Fig. 9 Visualization of boiling in non-anodized and anodized thermosiphon at different heat input a) 10 W b) 20W c) 30W d) 40W for fill ratio of 70%.

anodized thermosiphon. The maximum heat transfer coefficient at the evaporator of anodized thermosiphon is 3587 W/m^2 K and the same for the non-anodized thermosiphon is 2742 W/m^2 K. Therefore the enhancement in heat transfer coefficient of the anodized evaporator is 24% higher than that of the non-anodized thermosiphon. This variation may be due to the change in boiling dynamics from the anodizing effect. As can be seen in Fig. 9 (b,d,f,h) that a large number of bubble formation is witnessed due to the enhancement in the nucleation sites as shown in Fig 3(b) in the anodized thermosiphon. At low heat inputs, there is no bubble formation found in the non-anodized case (Fig.9a), and as the heat input increases there are few bubbles opened up in the corner of the evaporator (Fig.9c) or from the rough surface of evaporator though there were no artificial nucleation sites. Even though, the heat transfer occurs because of the evaporation process and this phenomenon is ensured by witnessing the condensate return from the condenser as shown in Fig 9. Further increase in heat input found to increase the intensity of bubble formation in the same nucleation sites (Fig 9 e & g). In the case of anodized thermosiphon, at low heat inputs, there are a large number of nucleations found as shown in Fig 9(b). As the heat input increases, it is seen that there is the formation of additional nucleations as well as an increase in boiling intensity (Fig 9 d). This phenomenon is witnessed from the increase in foam height, resulting from the intense boiling in the evaporator surface. It is observed that the increase in foam height is due to the expansion of vapor bubbles at the free surface of the working fluid, that is formed and raised from various locations of evaporator. So we can conclude from the visualization that the formation of additional nucleations and an increase in the intensity of boiling is responsible for the increase in heat transfer with anodized surface. Moreover, the bubble diameter in the anodized surface is roughly measured from the photographs and is about 525µm. However, there is no variation in bubble diameter observed in the current study though there is a significant variation is observed in the bubble frequency. However, no quantitative measurement was available regarding the bubble frequency, and more in-depth experimental studies are needed to explain quantitatively. Further, it is noticed that the maximum heat transfer coefficient

in the condenser of anodized and non-anodized thermosiphon is 2858 and 2488 W/m^2 K respectively. Though there is no coating provided in the condenser section, the heat transfer coefficient of anodized thermosiphon increased to 13% compared to that of the non-anodized thermosiphon. This enhancement of the heat transfer coefficient in the condenser is due to the heat transfer enhancement in the evaporator section. Heat transfer enhancement in the evaporator resulted from the higher rate of boiling leads to the increase in condensation rate since sufficient amount of cooling water is supplied to condense the entire vapor generated, leading to the effective circulation of heat transfer fluid in the thermosyphon and resulting in enhanced heat transfer coefficient. The condenser section of thermosyphon is also monitored during the heat transfer process. The condensation process is found to be quite different compared to the condensation of conventional fluids. In the present study, no droplet formation is seen or difficult to locate the droplets (too small to capture using the camera) in the condenser. However, a stream of liquid is seen flowing from the condenser to the evaporator. As the heat input increases the velocity of the liquid stream also increasing suggesting that the rate of condensation is increasing by the rate of boiling increase with an increase in heat input. Therefore the condenser heat transfer coefficient also increases.

Conclusions

Heat transfer characteristics of non-anodized flat thermosiphon were carried out with the fill ratio between 40% and 100%. Initially, the optimum fill ratio of non-anodized thermosiphon was found and was 70% of the evaporator volume. Performance comparison of anodized and non-anodized thermosiphon was made using the calculated heat transfer coefficients at the evaporator and condenser. The heat transfer coefficient at the evaporator of anodized thermosiphon is enhanced up to 24% compared to that of the non-anodized case. This enhancement in heat transfer coefficient results from the lower evaporator temperature for the same heat input as well as the boiling enhancement due to anodizing. The process of anodization creates more nucleation sites, and these

nucleation sites were activated at relatively lower heat input. The study confirmed the importance of nucleation sites as the heat transfer coefficient increased with the increase in a number of nucleation sites. Anodization is found to be an efficient, economical and relatively simple method for enhancing the heat transfer characteristics of thermosiphon.

ACKNOWLEDGMENT

The first author would like to thank the DST-SERB for financially assisting this research work under the project number YSS/2015/001084.

NOMENCLATURE

C : specific heat (J/kg K)
h : heat transfer coefficient (W/m^2 K)
T : temperature (^{o}C)
Q : heat transfer rate (W)
q : heat flux (W/m^2)
R : resistance (^{o}C/W)

SYMBOLS

c : condenser
e : evaporator
in : input
out : output
T : total
sat : saturated
v : vapor

REFERENCES

[1]. A.K. Das, P.K. Das, and Saha, Nucleate boiling of water from plain and structured surfaces, Exp. Therm. Fluid Sci. 31 (2007) 967–977.

[2]. L. Lu, Z.H. Liu, H.S. Xiao, Thermal performance of an open thermosiphon using nanofluids for high-temperature evacuated tubular solar collectors Part 1: Indoor experiment, Sol. Energy 85 (2011) 379–387.

[3]. S. Khandekar, Y. Joshi, B. Mehta, Thermal performance of closed two-phase thermosiphon using nanofluids", Int. J. Therm. Sci. 47 (2008) 659–667.

[4]. L. Vasiliev, L. Grakovich, M. Rabetsky, V. Romanenkov, L. Vasiliev Jr., V. Ayel, Yves Bertin, C. Romestant, J. Hugon, Grooved heat pipes with nanoporous deposit in an evaporator, Heat Pipe Sci. Tech. 1 (2010) (3) 219–236.

[5]. M. Rahimi, K. Asgary, S. Jesri, Thermal characteristics of a resurfaced condenser and evaporator closed two-phase thermosiphon, Int. Commun. Heat Mass Transf. 37, (2010) 703–710.

[6]. Teodori, A.S. Moita, A.L.N. Moreira, Characterization of pool boiling mechanisms over micro-patterned surfaces using PIV, Int. J. Heat Mass Transf. 66 (2013) 261–270

[7]. C. Y. Lee, Md M. H. Bhuiya, K. J. Kim, Pool boiling heat transfer with nano-porous surface. Int. J. Heat Mass Transf 53 (2010) 4274–4279.

[8]. G. U. Kumar, S. Suresh, M.R. Thansekhar, D. Babu, Effect of diameter of metal nanowires on pool boiling heat transfer with FC-72, Appl. Surf. Sci. 423 (2017) 509–520,

[9]. E. Demir, T. Izci, A.S. Alagoz, T. Karabacak, A. Koşar, Effect of silicon nanorod length on horizontal nanostructured plates in pool boiling heat transfer with water, Int. J. Therm. Sci. 82 (2014) 111–121.

[10]. R. Chen, M.C. Lu, V. Srinivasan, Z. Wang, H.H. Cho, A. Majumdar, Nanowires for enhanced boiling heat transfer, Nano Lett. 9 (2009) 548–553.

[11]. Z. Yao, Y.W. Lu, S.G. Kandlikar, Pool boiling heat transfer enhancement through nanostructures on silicon microchannels, J. Nanotechnol. Eng. Med. 3 (2013) 31002.

[12]. A. Surtaev, D. Kuznetsov, V. Serdyukov, A. Pavlenko, V. Kalita, D. Komlev, A. Ivannikov, A. Radyuk, Structured capillary-porous coatings for enhancement of heat transfer at pool boiling, Appl. Therm. Eng., 133 (2018) 532-542.

[13]. D. Deng, W. Wan, J. Feng, Q. Huang, Y. Qin, Y. Xie, Comparative experimental study on pool boiling performance of porous coating and solid structures with reentrant channels, Appl. Therm. Eng., 107 (2016) 420-430.

[14]. S.W. Ahmad , J.S. Lewis , R.J. McGlen and T.G. Karayiannis, Pool boiling on modified surfaces using R-123, Experimental Heat Transfer 35(2014)1491-1503

[15]. R. Khodabandeh, R. Furberg, Heat transfer, flow regime and instability of a nano- and micro-porous structure evaporator in a two-phase thermosiphon loop. Int. J. Therm. Sci. 49 (2010) 1183-1192.

[16]. D. V. Krishnan, G. U. Kumar, S. Suresh, M.R. Thansekhar, Uzair Iqbal, Evaluating the scale effects of metal nanowire coatings on the thermal performance of miniature loop heat pipe, Appl. Therm. Eng. 133 (2018) 727–738.

[17]. Q. Chen, Y. Huang, Scale effects on evaporative heat transfer in carbon nanotube wick in heat pipes, Int. J. Heat Mass Transf. 111 (2017) 852–859.

[18]. W. Ling, W. Zhou, R. Liu, Q. Qiu, Y. Ke, Operational characteristics of loop heat pipes with porous copper fiber sintered sheet as wick, Appl. Therm. Eng. 122 (2017) 398–408.

[19]. C. Buffone, J. Coulloux, B. Alonso, M. Schlechtendahl, V. Palermo, A. Zurutuza, T. Albertin, S. Martin, M. Molina, S. Chikov, R. Muelhaupt, Capillary pressure in graphene oxide nanoporous membranes for enhanced heat transport in Loop Heat Pipes for aeronautics, Exp. Therm. and Fluid Sci. 78 (2016) 147–152.

[20]. J. Choi, Y.Yuan, WataruSano, D.A. Borca-Tasciuc, Low temperature sintering of copper biporous wicks with improved maximum capillary pressure, Mater. Lett. 132 (2014) 349-352.

[21]. C. Y. Lee, B. J. Zhang, K. J. Kim, Morphological change of plain and nano-porous surfaces during boiling and its effect on nucleate pool boiling heat transfer. Exp. Therm. and Fluid Sci. 40 (2012) 150–158.

[22]. A. B. Solomon, A. Mathew, K. Ramachandran, B.C. Pillai, V.K. Karthikeyan "Thermal performance of anodized two phase closed thermosiphon (TPCT)." Exp. Therm. and Fluid Sci. 48 (2013) 49–57.

[23]. A. B. Solomon, R. Roshan, W. Vincent, V. K. Karthikeyan, L. G. Asirvatham, Heat transfer performance of an anodized two-phase closed thermosyphon with refrigerant as working fluid, Int. J. Heat Mass Transf. 82 (2015) 521-529.

[24]. R. R. Singh, V. Selladurai, P.K. Ponkarthik, A. B. Solomon, Effect of anodization on the heat transfer performance of flat thermosyphon, Exp. Therm. Fluid Sci. 68 (2015) 574–581.

[25]. A. B. Solomon, A. M. R. Kumar, K. Ramachandran, B. C. Pillai , C. S. Kumar, M. Sharifpur, J. P. Meyer, Characterisation of a grooved heat pipe with an anodized surface, Heat Mass Transf. 53(3) (2017) 753-763.

[26]. A. B. Solomon, V. A. Daniel, K. Ramachandran, B.C. Pillai, R. R. Singh, M. Sharifpur, J.P. Meyer, Performance enhancement of a two-phase closed thermosiphon with a thin porous copper coating, Int. Commun. Heat Mass Transf. 82 (2017) 9-19.

[27]. C.Y. Lee, M.M.H. Bhuiya, K.J. Kim, Pool boiling heat transfer with nanoporous surface, Int. J. Heat Mass Transfer 53 (2010) 4274–4279.